Journal of Biomolecular Structure and Dynamics

ISSN: (Print) (Online) Journal homepage: www.tandfonline.com/journals/tbsd20

Effects and molecular mechanisms of the combination of *Andrographis paniculata* and *Anredera cordifolia* as an insulin sensitizer: *in vitro*, network pharmacology, molecular docking, and dynamics studies

Frangky Sangande, Sri Ningsih, Kurnia Agustini, Siska Andrina Kusumastuti, Nuralih Nuralih, Adam Arditya Fajriawan, Michael Chandra, Syofi Rosmalawati, Aiyi Asnawi & Krisyanti Budipramana

To cite this article: Frangky Sangande, Sri Ningsih, Kurnia Agustini, Siska Andrina Kusumastuti, Nuralih Nuralih, Adam Arditya Fajriawan, Michael Chandra, Syofi Rosmalawati, Aiyi Asnawi & Krisyanti Budipramana (06 May 2025): Effects and molecular mechanisms of the combination of *Andrographis paniculata* and *Anredera cordifolia* as an insulin sensitizer: *in vitro*, network pharmacology, molecular docking, and dynamics studies, Journal of Biomolecular Structure and Dynamics, DOI: 10.1080/07391102.2025.2499224

To link to this article: https://doi.org/10.1080/07391102.2025.2499224

Published online: 06 May 2025.

JOURNAL OF BIOMOLECULAR STRUCTURE AND DYNAMICS
https://doi.org/10.1080/07391102.2025.2499224

Taylor & Francis
Taylor & Francis Group

Effects and molecular mechanisms of the combination of *Andrographis paniculata* and *Anredera cordifolia* as an insulin sensitizer: *in vitro*, network pharmacology, molecular docking, and dynamics studies

Frangky Sangande[a], Sri Ningsih[a], Kurnia Agustini[a], Siska Andrina Kusumastuti[a], Nuralih Nuralih[a], Adam Arditya Fajriawan[a], Michael Chandra[b], Syofi Rosmalawati[c], Aiyi Asnawi[d], and Krisyanti Budipramana[e]

[a]Research Center for Pharmaceutical Ingredients and Traditional Medicine, National Research and Innovation Agency (BRIN), Cibinong Science Center, Bogor, Indonesia; [b]SOHO Industri Pharmasi, East Jakarta, Indonesia; [c]Research Center for Applied Microbiology, National Research and Innovation Agency (BRIN), Cibinong Science Center, Bogor, Indonesia; [d]Faculty of Pharmacy, Universitas Bhakti Kencana, Bandung, Indonesia; [e]Department of Pharmaceutical Biology, Faculty of Pharmacy, University of Surabaya, Surabaya, Indonesia

ABSTRACT

Due to the complex mechanism of insulin resistance (IR), multi-component herbal medicines might be an alternative approach in the treatment of IR-related diseases, such as type 2 diabetes mellitus (T2DM). *Andrographis paniculata* (AP) and *Anredera cordifolia* (AC) have been reported to have anti-diabetic effects. However, their effect and mechanism of action in a mixed formula (FAPAC), especially as an insulin sensitizer have not been reported. Therefore, *in vitro* studies were performed to investigate the effect of FAPAC, and the molecular mechanisms were predicted by in silico studies through network pharmacology, molecular docking, and dynamics simulations. *In vitro* studies demonstrated that FAPAC at 2 μg/mL was comparable to metformin in increasing glucose uptake in IR-HepG2 cells. KEGG analysis revealed that IR was the top pathway and predicted that FAPAC acts as an insulin-sensitizing agent by inhibiting three main targets: IKBKB, PRKCD, and PTPN1. Consensus docking suggested 7-O-methyl wogonin, ninandrographolide, and 3-O-β-D-glucopyranosyl andrographolide as the potent inhibitors for IKBKB, PRKCD, and PTPN1, respectively. Furthermore, molecular dynamics confirmed that the potential compounds remained in the binding pocket throughout the simulation and had a good affinity toward their respective targets, comparable to native ligands.

ARTICLE HISTORY
Received 30 November 2023
Accepted 27 August 2024

KEYWORDS
Andrographis paniculata; *Anredera cordifolia*; extract combination; molecular mechanism; insulin resistance

1. Introduction

IR plays a vital role in the pathogenesis of type 2 diabetes mellitus (T2DM) (Galicia-Garcia et al., 2020). This condition causes the failure of primary target tissues, such as muscle, liver, and adipose tissue to correctly respond to insulin activity triggering an increase in blood glucose levels (Lee et al., 2022). IR is a complex mechanism including several upstream and downstream signaling molecules in insulin signal transduction (Mengwei Li et al., 2022; Urzua et al., 2019). Moreover, extracellular factors including immune abnormalities, lipotoxicity, hypoxic environments, and inflammation, have also been reported to trigger IR by inducing intracellular stress (Zhao, An, et al., 2023). Current anti-hyperglycemic medicines such as thiazolidinediones, sodium-glucose cotransporter (SGLT)-2 inhibitors, and metformin have been used to improve IR by targeting different key molecules (Mastrototaro & Roden, 2021). For patients who do not respond well to monotherapy, these anti-hyperglycemic medicines combination can be recommended. For instance, a combination of rosiglitazone with metformin resulted in better IR improvement than metformin alone (Arslanian et al., 2013), demonstrating the important role of multi-target therapy in IR treatment.

In addition to conventional anti-hyperglycemic medicines, multi-component herbal medicines can modulate one or more pathways that regulate IR (Chang et al., 2013). Several studies have demonstrated the use of herbal medicines as a potential source of multi-target anti-IR. *Morus alba* leaf extract has been reported as an anti-IR by targeting IRS-1 and JNK (Liu et al., 2016). *Toona sinensis* leaf showed insulin-sensitizing effects by modulating AMPK and PPARγ (Liu et al., 2015). *Momordica charantia* improves IR through the inhibition of NF-κB and JNK pathways (Yang et al., 2015).

AP and AC as a single herb have been reported to exhibit anti-diabetic effects based on *in vitro* and *in vivo* studies (Suemanotham et al., 2023; Sulfianti et al., 2023). There are, to our knowledge, no previous studies concerning the effect and mechanism of AP and AC combination in IR treatment. In certain cases, herb combinations exhibited a superior effect than a single herb by improving pharmacokinetic, pharmacodynamic, and toxicity profiles (Sangande et al., 2023). A study revealed that there was a better increase in

CONTACT Frangky Sangande frangky.sangande@gmail.com, fran015@brin.go.id Research Center for Pharmaceutical Ingredients and Traditional Medicine, National Research and Innovation Agency (BRIN), Cibinong Science Center, Bogor, Indonesia

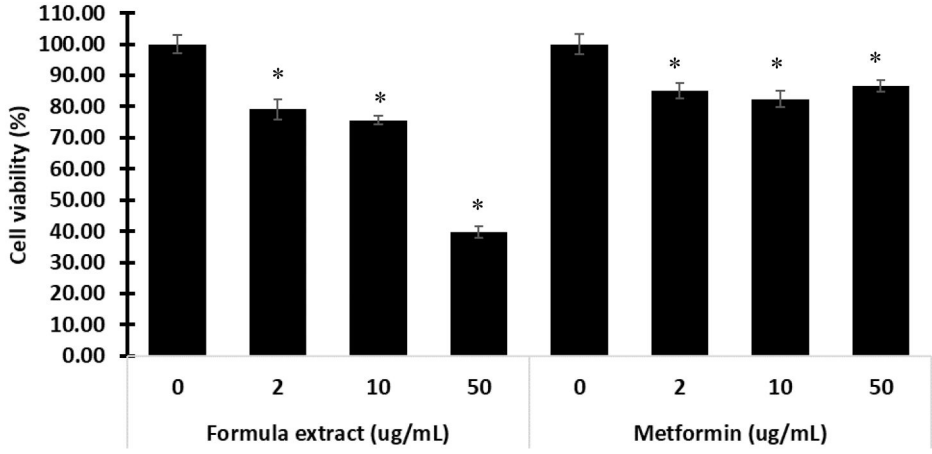

Figure 1. Cytotoxicity test of FAPAC on HepG2 cells. Values are provided as means ± SD from three independent experiments. (*) difference significantly was compared to untreated cells ($p < .05$).

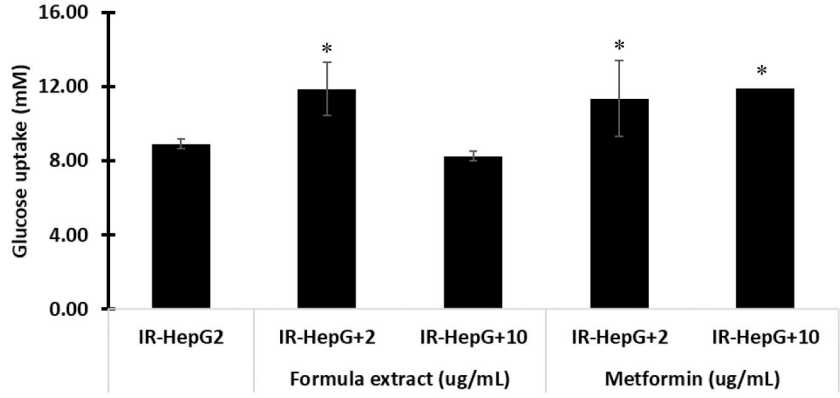

Figure 2. Glucose uptake on IR-HepG2 cells after FAPAC treatment. Values are the mean ± SD. (*) different significantly from the IR model ($p < .05$).

insulin sensitivity when using a combination of *Scutellaria baicalensis* (radix) and *Coptis chinensis* (rhizoma) in ratio1:1 compared to a single herb (Cui et al., 2018).

Herbal medicines contain a large number of bioactive compounds in varying amounts that interact with each other through antagonistic, additive, or synergistic effects to result in biological activities (Vaou et al., 2022). The complexity of IR pathogenesis and the compound contained in herbal medicine provides a challenge in the mechanism of action elucidation. Fortunately, many studies have shown the power of network pharmacology combined with molecular docking to systematically predict the potential targets and compounds of herbal medicine (Bai et al., 2022; Zhao, Zhang, et al., 2023; Zhao, Fu, et al., 2023), as a reference before conducting expensive and time-consuming experimental studies for molecular mechanism elucidation. In the current study, therefore, the insulin-sensitizing effect of FAPAC was determined in IR-HepG2 cells by using metformin as the control. Afterward, we applied network pharmacology, molecular docking, and molecular dynamics (MD) simulations to predict the mechanism of action of FAPAC against IR. This study provides a scientific foundation for designing further experimental studies to obtain comprehensive results, especially in selecting targets to be tested.

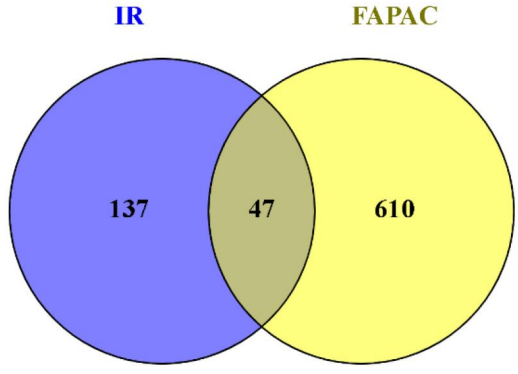

Figure 3. Venn diagram illustrating the common target between IR-related targets and FAPAC-related targets.

2. Materials and methods

2.1. Plant extraction

2.1.1. Plant collection and authentication

Dried AP herbs were bought from the local market in Yogyakarta and fresh AC leaves were from BRIN plantation in Lampung. Both plants were authenticated by the Research Centre for Biology, Indonesian Institute of Science (No. 493/IPH.1.01/If.07/II/2017).

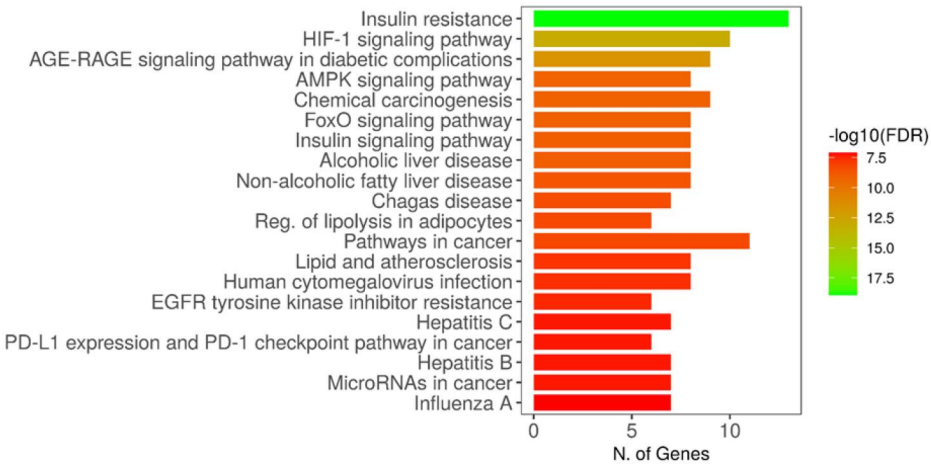

Figure 4. KEGG enrichment pathways.

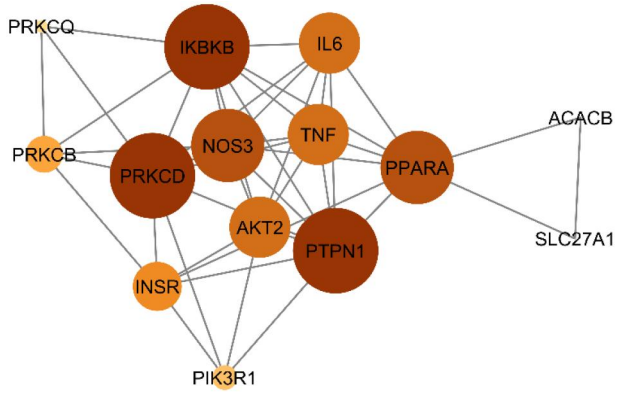

Figure 5. PPI network of 14 targets involved in the IR pathway. IKBKB, PRKCD, and PTPN1 are shown in darker and larger nodes, indicating a high degree level.

Table 1. Topology parameters of the main targets.

	Topology parameters					
Target	DC	EC	LAC	BC	CC	NC
IKBKB	9	0.4	4.9	18.5	0.8	7.5
PRKCD	9	0.3	4.0	14.0	0.7	6.8
PTPN1	9	0.4	5.3	9.8	0.8	7.9
Cutoff	6	0.2	3.4	8.3	0.6	4.8

2.1.2. Preparation of extracts

Dried AP was ground into powder and then extracted using ethanol with maceration for 4 h. The filtrate was evaporated using a vacuum evaporator (50 °C) to obtain semisolid mass. A similar extraction procedure was conducted on AC leaves after being dried and milled into powder. Each semisolid extract was then mixed in the proportional combination until a homogeneous mass was obtained and kept in the amber bottle for the next experiment. The extract combination was termed FAPAC.

2.2. In vitro study

2.2.1. Cellular assay

The HepG2 (human hepatocarcinoma) cell lines were obtained from the Laptiab laboratory-BRIN collection. Dulbecco's modified Eagle's medium (DMEM) containing 10% Fetal Bovine Serum (FBS) and 1% penicillin/streptomycin (PS, 100 units of penicillin/mL and 100 pg streptomycin/mL) was used to maintain cells. The cells were incubated at 37 °C, 5% CO_2, and replacing the medium every 48 h.

2.2.2. Cells viability assay

The cytotoxicity test using 3-[4,5-dimethylthiazol-2-yl]-2,5 diphenyl tetrazolium bromide (MTT) was performed based on a previous study (Mosmann, 1983). The HepG2 cells were seeded in 96-well plates at a density of 1.0 × 104 cells/well. After being incubated for 24 h, cells were treated by FAPAC in various concentrations (2, 10, and 50 µg/mL) for 24 h. Afterward, the medium was removed, cells were washed with PBS and 100 µL of MTT (0.5 mg/mL) was added followed by incubation for 4 h. Subsequently, cells were incubated overnight in 100 µL solution containing 10% sodium dodecyl sulfate (SDS) in 0.1 N HCl to determine the number of living cells by measuring the absorbance of the medium at 570 nm using a microplate reader (Synergy HTX; Bio-Tek Instruments Inc., Winooski, VT, USA). The percentage of viable cells in each concentration was determined relative to the group without treatment. The non-toxic concentrations were used in the further experiment.

2.2.3. Cellular glucose uptake assay

IR-HepG2 cells were developed with slight modifications based on previous papers (Hu et al., 2014; Mosmann, 1983; Panahi et al., 2018). Briefly, HepG2 cells were cultured in 96-well plates at a density of 3.0 × 104 until 80%–90% confluency. After that, the medium was replaced with serum-free DMEM supplemented with 30 mM glucose concentration, and cells were re-incubated for the next 24 h. Furthermore, cells were treated with various concentrations of FAPAC and standard metformin (2 and 10 µg/mL) in serum-free DMEM for 24 h followed by another incubation for 30 min in serum-free DMEM supplemented with 1 µg/mL insulin (Sigma Aldrich, Saint Louis, USA). The glucose content within each medium was quantified utilizing the Glucose GOD-PAP kit assay (Diasys Diagnostics, Holzheim, Germany). The glucose uptake value was calculated by subtracting the glucose

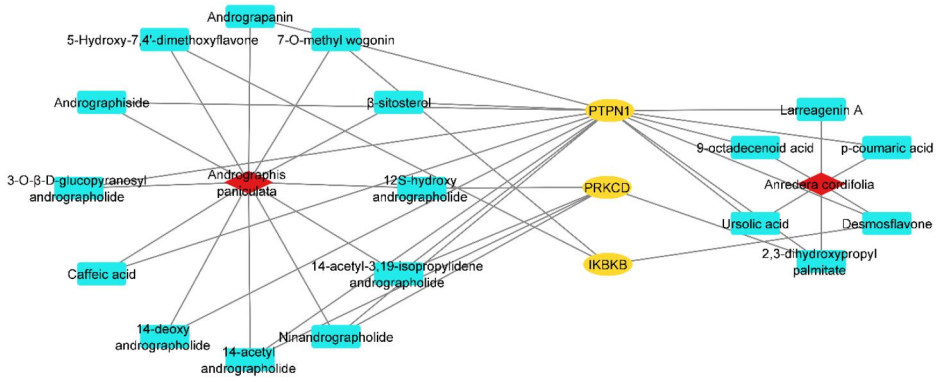

Figure 6. Herb-compound-target network.

Table 2. Comparison of the redocking pose and crystallography pose of native ligands.

Target	DOCK6	Vina
IKBKB		
PRKCD		
PTPN1		

Table 3. The score of duplet conformation on main targets using DOCK6.

	DOCK6 score		
Compound	IKBKB	PRKCD	PTPN1
14-acetyl-3,19-isopropylidene andrographolide	−55.4	−35.1	–
2,3-dihydroxypropyl palmitate	–	–	–
5-hydroxy-7,4′-dimethoxyflavone	−53.7	–	−44.6
12S-hydroxy andrographolide	−47.7	−37.9	–
7-O-methyl wogonin	−54.3	−34.8	−38.9
Ninandrographolide	–	−45.4	–
Ursolic acid	–	−33.9	–
Larreagenin A	−36.7	−31.2	–
Desmosflavone	–	–	–
9-octadecenoid acid	–	–	–
14-acetyl andrographolide	−46.0	−40.4	–
β-sitosterol	−53.4	−35.4	–
Andrograpanin	−48.8	–	–
Andrographiside	–	−45.1	–
Caffeic acid	−34.2	–	−36.1
p-Coumaric acid	−34.0	–	−35.4
3-O-β-D-glucopyranosyl andrographolide	–	–	−57.8
14-deoxy andrographolide	−50.9	−38.1	−41.7
Native ligand of IKBKB	−78.6		
Native ligand of PRKCD		−44.7	
Native ligand of PTPN1			−44.6

Table 4. The score of duplet conformation on main targets using Vina.

	Vina score		
Compound	IKBKB	PRKCD	PTPN1
14-acetyl-3,19-isopropylidene andrographolide	−7.8	−5.0	–
2,3-dihydroxypropyl palmitate	–	–	–
5-hydroxy-7,4′-dimethoxyflavone	−9.4	–	−7.1
12S-hydroxy andrographolide	−7.4	−4.8	–
7-O-methyl wogonin	−9.0	−5.6	−6.2
Ninandrographolide	–	−5.5	–
Ursolic acid	–	−5.4	–
Larreagenin A	−6.2	−5.7	–
Desmosflavone	–	–	–
9-octadecenoid acid	–	–	–
14-acetyl andrographolide	−7.1	−5.4	–
β-sitosterol	−8.8	−4.7	–
Andrograpanin	−8.3	–	–
Andrographiside	–	−5.3	–
Caffeic acid	−6.8	–	−6.9
p-Coumaric acid	−6.7	–	−6.9
3-O-β-D-glucopyranosyl andrographolide	–	–	−7.9
14-deoxy andrographolide	−7.6	−5.3	−6.2
Native ligand of IKBKB	−12.4		
Native ligand of PRKCD		−5.8	
Native ligand of PTPN1			−8.3

concentration in treated cells from the blank wells (medium only).

2.3. Statistical analysis

All data was performed in an average ± SD. Statistical analysis was performed using SPSS 13 program. The difference between groups was compared using One-way analysis of variance (ANOVA) for parametric data followed by LSD post hoc test and for non-parametric data analyzed using Kruskal Wallis followed with Mann Whitney test post hoc. The statistically significant difference was defined as a *p*value of less than .05 ($p < .05$).

2.4. Active compounds search and potential targets of FAPAC

Active compounds of AP herb and AC leaf were collected from the KNApSAcK database and literature search on

Pubmed and Google Scholar. Furthermore, by using their SMILES submitted to SwissTargetPrediction (http://www.swisstargetprediction.ch/), we predicted the potential targets (probability value $\geq$ 0.1) of these compounds.

2.5. Collection of IR-related targets of FAPAC

Comparative Toxicogenomics Database (CTD) (http://ctdbase.org/) and DisGeNet (https://www.disgenet.org/) were used to collect for IR-related targets. In CTD we used 'insulin resistance' as the keyword and only targets marked as 'marker/mechanism' and/or 'therapeutic' were selected. In DisGeNet, all targets included in the search using the keyword 'insulin resistance' (CUI: C0021655) were selected. After deleting the duplicate targets from the two databases, we overlaid the potential targets of FAPAC with these IR-related targets using the Venny 2.1 tool (https://bioinfogp.cnb.csic.es/tools/venny/index.html). The common targets were considered IR-related targets of FAPAC.

2.6. KEGG analysis

ShyniGO 0.77 (http://bioinformatics.sdstate.edu/go/) was used to analyze KEGG enrichment at the p value of $\leq$ .05 after importing the IR-related targets of FAPAC into this tool. The top 20 enriched pathways ranked by false discovery rate (FDR) were obtained. Because our study is focused on IR, we only retrieved targets from this pathway for further protein-protein interaction (PPI) analysis.

2.7. Construction of PPI network of targets from IR pathway

All targets included in the IR pathway were submitted to the STRING database (https://string-db.org/) and constructed their PPI network. The confidence parameter was set to 0.7 in *Homo sapiens*. The results were imported to Cytoscape 3.9.3 for topology calculation including local average connectivity (LAC), closeness centrality (CC), degree centrality (DC), eigenvector centrality (EC), betweenness centrality (BC), and network centrality (NC) using the CytoNCA plugin. The mean value of every topology parameter was calculated and used as a cutoff. Targets with topology values more than the cutoff were considered the main targets for further docking simulations.

2.8. Identification of potential compounds through molecular docking

For docking simulation, we rescreened compounds that have at least one of the main targets generated from SwissTargetPrediction. The 3D structure of these compounds was retrieved from PubChem. The structures of the main targets: IKBKB (PDB:4KIK), PRKCD (PDB: 1PTR), and PTPN1 (PDB: 1C83) were downloaded from RCSB. DOCK6 (Allen et al., 2015) and Vina (Trott & Olson, 2010) were used for docking simulations and the protocols were developed based on a previous study (Sangande et al., 2023).

In DOCK6, the AM1-BBC method was used for adding the charges to the targets and ligands. The molecular surface was generated by using a probe radius of 1.4 Å. Spheres within 8 Å of the native ligand with an extra margin of 5 Å were used for defining the active site.

In Vina, the targets were prepared by adding polar hydrogen atoms and Kollman charges, while the ligands were added with Gestaiger charges. The grid box sizes of $22 \times 22 \times 22$ Å for IKBKB and PRKCD, and $18 \times 18 \times 18$ Å for PTPN1, at a spacing of 1 Å, were centered on their respective native ligand position to obtain the center coordinate.

The two docking protocols were set to generate 10 conformations per ligand to be compared with each other. Only compounds with a duplet conformation detected in DOCK6 and Vina were calculated for their consensus score (mean value of the scores of these conformations). The potential

Table 5. Consensus score of duplet conformation on main targets.

	Consensus score		
Compound	IKBKB	PRKCD	PTPN1
14-acetyl-3,19-isopropylidene andrographolide	−31.6	−20.1	–
2,3-dihydroxypropyl palmitate	–	–	–
5-hydroxy-7,4′-dimethoxyflavone	−31.6	–	−25.9
12S-hydroxy andrographolide	−27.6	−21.4	–
7-O-methyl wogonin	**−31.7**	−20.2	−22.6
Ninandrographolide	–	**−25.5**	–
Ursolic acid	–	−19.7	–
Larreagenin A	−21.5	−18.5	–
Desmosflavone	–	–	–
9-octadecenoid acid	–	–	–
14-acetyl andrographolide	−26.6	−22.9	–
β-sitosterol	−31.1	−20.1	–
Andrograpanin	−28.6	–	–
Andrographiside	–	25.2	–
Caffeic acid	−20.5	–	−21.5
p-Coumaric acid	−20.4	–	−21.2
3-O-β-D-glucopyranosyl andrographolide	–	–	**−32.8**
14-deoxy andrographolide	−29.3	−21.7	−23.8
Native ligand of IKBKB	−45.5		
Native ligand of PRKCD		−25.3	
Native ligand of PTPN1			−26.5

Table 6. Binding free energy of ligand-target complexes.

	Energy (Kcal/mol)						
Ligand	ΔVDWAALS	ΔEEL	ΔEGB	ΔESURF	ΔGGAS	ΔGSOLV	ΔTOTAL
7-O-methyl wogonin-IKBKB	−34.36	−8.79	20.51	−4.49	−43.15	16.02	−27.13
Native ligand-IKBKB	−32.63	−5.13	12.32	−3.48	−37.77	8.85	−28.92
Ninandrographolide-PRKCD	−32.60	−6.92	17.27	−4.60	−39.52	12.67	−26.85
Native ligand-PRKCD	−31.21	−12.05	18.81	−3.77	−43.26	15.04	−28.22
3-O-β-D-glucopyranosyl andrographolide-PTPN1	−26.61	−5.44	18.50	−3.84	−32.06	14.66	−17.39
Native ligand-PTPN1	−22.23	−4.57	14.36	−3.17	−26.80	11.19	−15.61

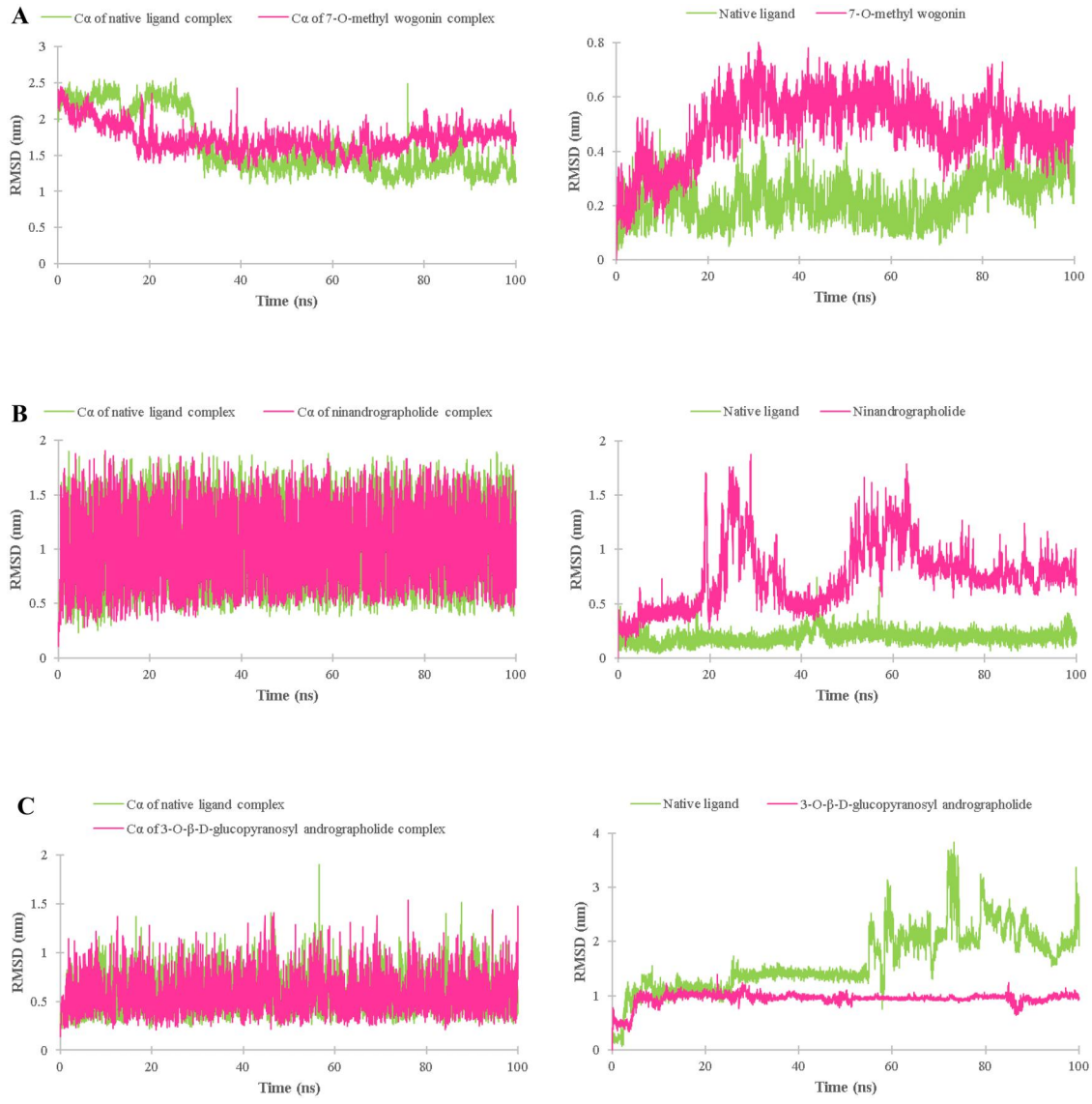

Figure 7. Backbone (Cα) and ligand RMSD profiles of IKBKB complexes (A); PRKCD complexes (B); PTPN1 complexes (C).

compounds of FAPAC were defined as compounds showing the best consensus score.

2.9. Molecular dynamics simulations and binding free energy analysis

MD simulations were performed using Gromacs 2023.1 (Hess et al., 2008). The topologies of potential compounds and native ligands were prepared using ACPYPE 2022.6.6 while for the target topologies, AMBER99SB-ILDN was used as the force field parameters. TIP3P water model was used to dissolve the systems which was then neutralized by adding Na^+ or Cl^- ions. After minimization using the steepest descent method under 1000 kcal/mol/nm, the systems were then equilibrated using 250 ps NVT (constant number of particles, volume, and temperature) ensemble at 310°K, and 250 ps NPT (constant number of particles, pressure, and temperature) at 1 bar. The production run was conducted for 100 ns. Subsequently, the binding free energy calculations were performed using gmx_MMPBSA 1.6.1, analyzing frames from 1 to 9,999,999 with an interval of 20 frames using the Generalized Born Surface Area (GBSA) method.

3. Results and discussion

3.1. In vitro study

Before testing the insulin-sensitizing effect of FAPAC, we evaluated the cell toxicity of this formula. HepG2 cells were treated with a range concentration of FAPAC (2, 10, and 50 μg/mL). FAPAC up to 10 μg/mL exhibited more than 80% cells viable relative to untreated cells and started to decline significantly at a concentration of 50 μg/mL (Figure 1). This result revealed that FAPAC was a safe and non-toxic agent in HepG2 up to 10 μg/mL.

To examine the glucose uptake effect, we incubated the IR cells with the FAPAC and metformin in various concentrations (2 and 10 μg/mL) for 24 h in a serum-free DMEM medium. FAPAC, especially at a concentration of 2 μg/mL

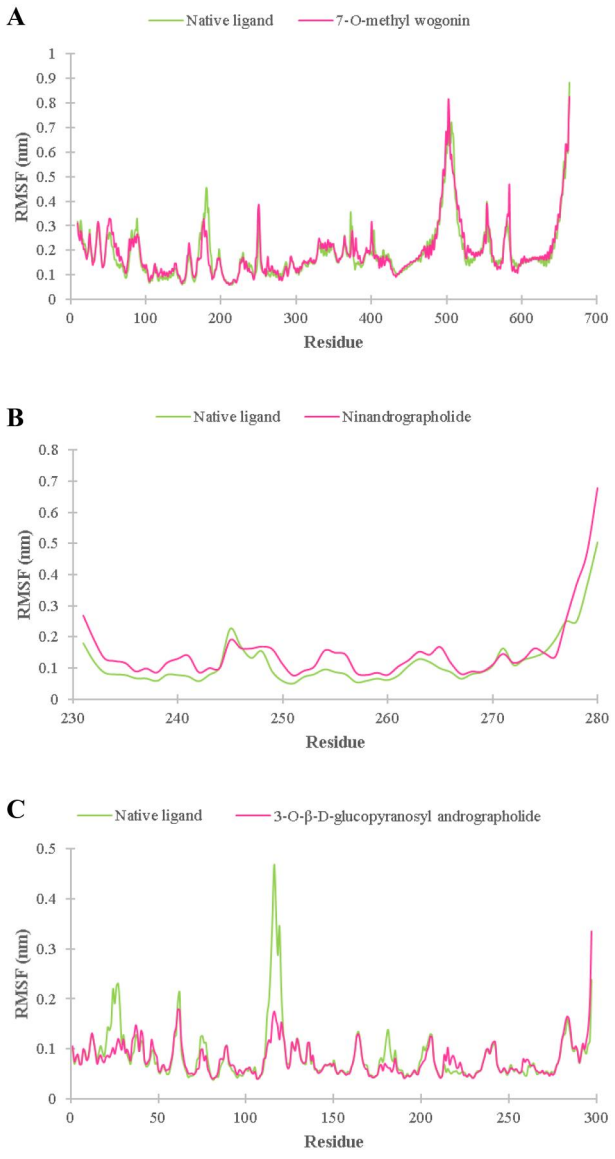

Figure 8. The RMSF profiles of IKBKB complexes (A); PRKCD complexes (B); PTPN1 complexes (C).

(IR-HepG + 2), significantly increased glucose uptake in IR-HepG2 cells compared to control IR-HepG2 cells ($p < .05$) (Figure 2). However, treating IR-HepG2 cells with 10 µg/mL of FAPAC (IR-HepG + 10) did not improve the glucose uptake of IR-HepG2 cells. On the other hand, metformin, as a standard oral diabetic drug for IR conditions, repaired the IR of the cells. All tested concentrations of metformin increase glucose uptake significantly compared to the model ($p < .05$) in a dose-dependent manner. Figure 2 also showed that the activities of FAPAC at 2 µg/mL and metformin were comparable, making this formula interesting for further study regarding the molecular mechanisms as presented in the results below.

3.2. Active compounds collection and IR-related target of FAPAC

After collecting the active compounds from the literature and database, and importing them into SwissTargetPrediction, we obtained 54 compounds contained in FAPAC that have 657 potential targets with a probability ≥ 0.1. However, their IR-related targets still need to be determined. Therefore, we collected 184 IR(disease)-related targets after merging and deleting duplicate targets from CTD and DisGeNet databases. Afterward, it was mapped to the 657 compound-related targets. Figure 3 revealed that only 47 targets were predicted as the IR-related target of FAPAC.

3.3. KEGG analysis and identification of potential targets

For further investigation, these 47 IR-related targets were submitted to ShyniGO for KEGG analysis, and we identified IR as the top pathway (Figure 4). In this pathway, there were 14 contributed targets, and their PPI network was constructed using STRING (Figure 5). From this PPI, we identified 3 main targets: IKBKB, PRKCD, and PTPN1 which have topological parameter values above the average (Table 1). IKBKB, PRKCD, and PTPN1 are the genes coding for IKK-β, PKC-δ, and PTP1B proteins, respectively. Inhibition of the activity of these proteins has been reported to ameliorate IR (Arkan et al., 2005; Mengyao Li et al., 2015; Ma et al., 2011).

3.4. Identification of potential compounds through molecular docking

From SwissTargetPrediction, we sorted out 12 compounds and 6 compounds were from AP and AC, respectively, which attacked at least one of the 3 main targets. Figure 6 revealed that the active compounds from AP and AC contribute to the inhibition of the three main targets, supporting the rationale for using the combination of these two herbs.

SwisTargetPrediction works based on similarity search, a ligand-based virtual screening (LBVS) method, assuming that structurally similar compounds may have a similar target (Gfeller et al., 2014). Combining LBVS with structure-based virtual screening (SBVS) such as molecular docking can increase the accuracy of the screening results (Oliveira et al., 2023). Moreover, molecular docking has been used in many network pharmacology studies to validate the results in addition to *in vitro* and *in vivo* which are feasible methods, but high-cost and time-consuming (Noor et al., 2022). Therefore, docking simulation was performed in the present study to initially validate the binding ability of the compounds to IKBKB, PRKCD, and PTPN1 proteins before validating these results using *in vitro* and *in vivo* in subsequent studies. Prior to docking simulation, the protocols of DOCK6 and Vina were validated, and Table 2 revealed that our docking protocols were valid, resulting in re-docking poses with a root-mean-square deviation (RMSD) value of <2 Å.

Many docking tools are currently available, and each tool may have a different algorithm and scoring function, thus their hit compounds may also differ. Even though they are the same, the docking pose can be different. Therefore, in the present study, we applied consensus docking where compounds without a duplet conformation detected in DOCK6 and Vina could be neglected because their pose is

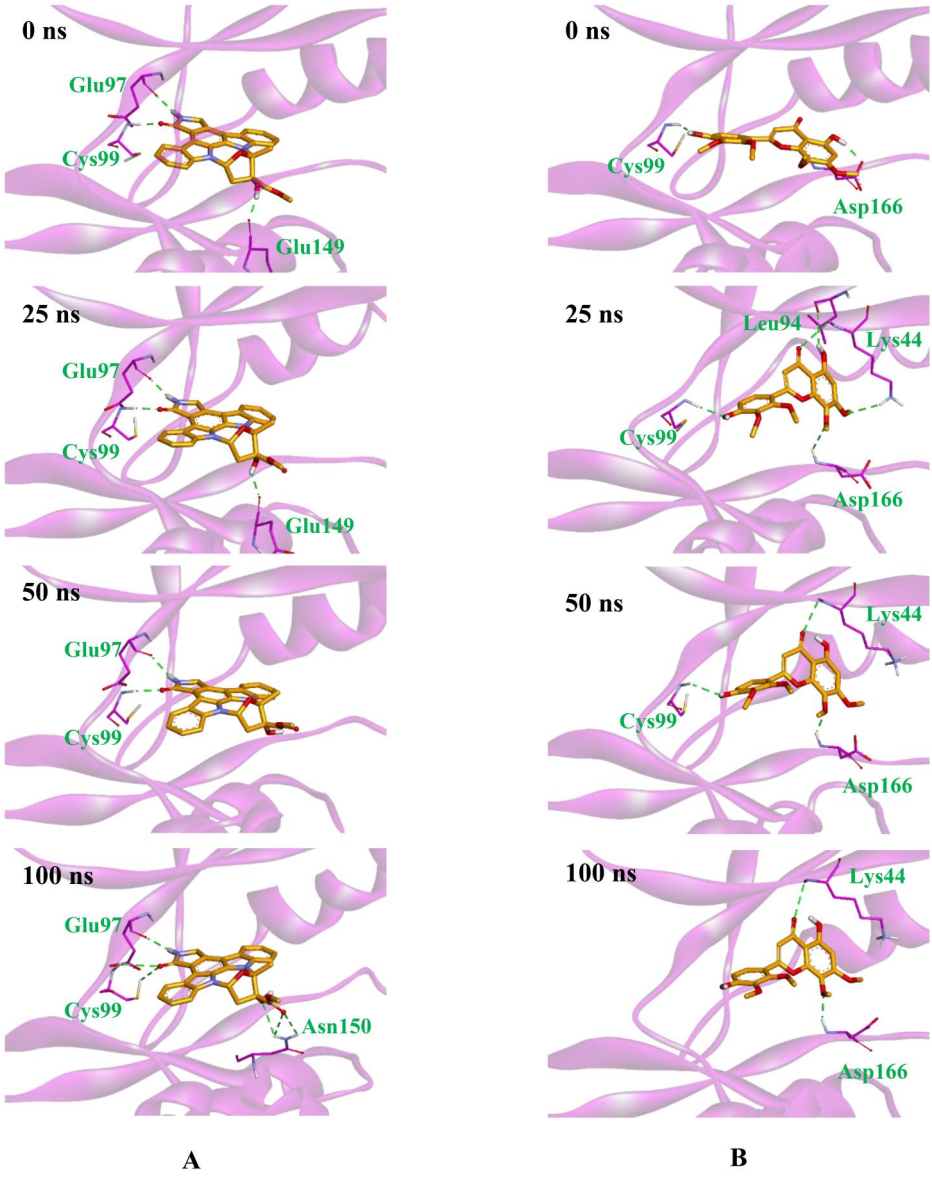

Figure 9. Interaction profiles of native ligand (A) and 7-O-methyl wogonin (B) on IKBKB during MD simulations.

suspicious (Ng et al., 2021). These compounds were not scored as shown in Tables 3 and 4. Consensus docking results (Table 5) suggested the three best-socred compounds of AP: 7-O-methyl wogonin, ninandrographolide, and 3-O-β-D-glucopyranosyl andrographolide as the most potent inhibitors for IKBKB, PRKCD, and PTPN1 respectively.

Some literature supported that these potential compounds might be active at the targets mentioned above. 7-O-methyl wogonin is a derivate of wogonin by substituting the hydroxyl group at C-7 with methoxy. A study demonstrated that wogonin has an anti-inflammatory effect by inhibiting phosphorylation of IKBKB thus suppressing NF-κB activation (Yao et al., 2014). 3-O-β-D-glucopyranosylandrographolide is one of the active compounds of AP. The extract of AP has been reported to inhibit PTPN1 activity with IC_{50} 13.4 μg/mL (Singh et al., 2022). PTPN1 is a key negative regulator of insulin signaling transduction by hydrolyzing tyrosine phosphorylation of insulin receptors and IRS-1 induced by insulin action, leading to decreased glucose uptake (Panzhinskiy et al., 2013). Meanwhile, no reports indicated the inhibitory activity of ninandrographolide or AP against PRKCD. However, andrographolide, a main compound of AP, was known to interfere with the activity of phorbol-12-myristate-13-acetate (PMA), an activator of PKC (Burgos et al., 2020). The rise in PRKCD activation will inhibit insulin signaling because it will increase Ser phosphorylation on insulin receptor and/or IRS-1, thus interfering with Tyr phosphorylation on IRS-1 mediated by insulin receptor (Shehadeh et al., 2021).

3.5. Molecular dynamics and binding free energy of potential compounds

Due to the simplification of molecular docking by ignoring several important parameters such as solvation effects and flexibility (Pantsar & Poso, 2018), MD simulations were performed to study the dynamic behavior and stability of

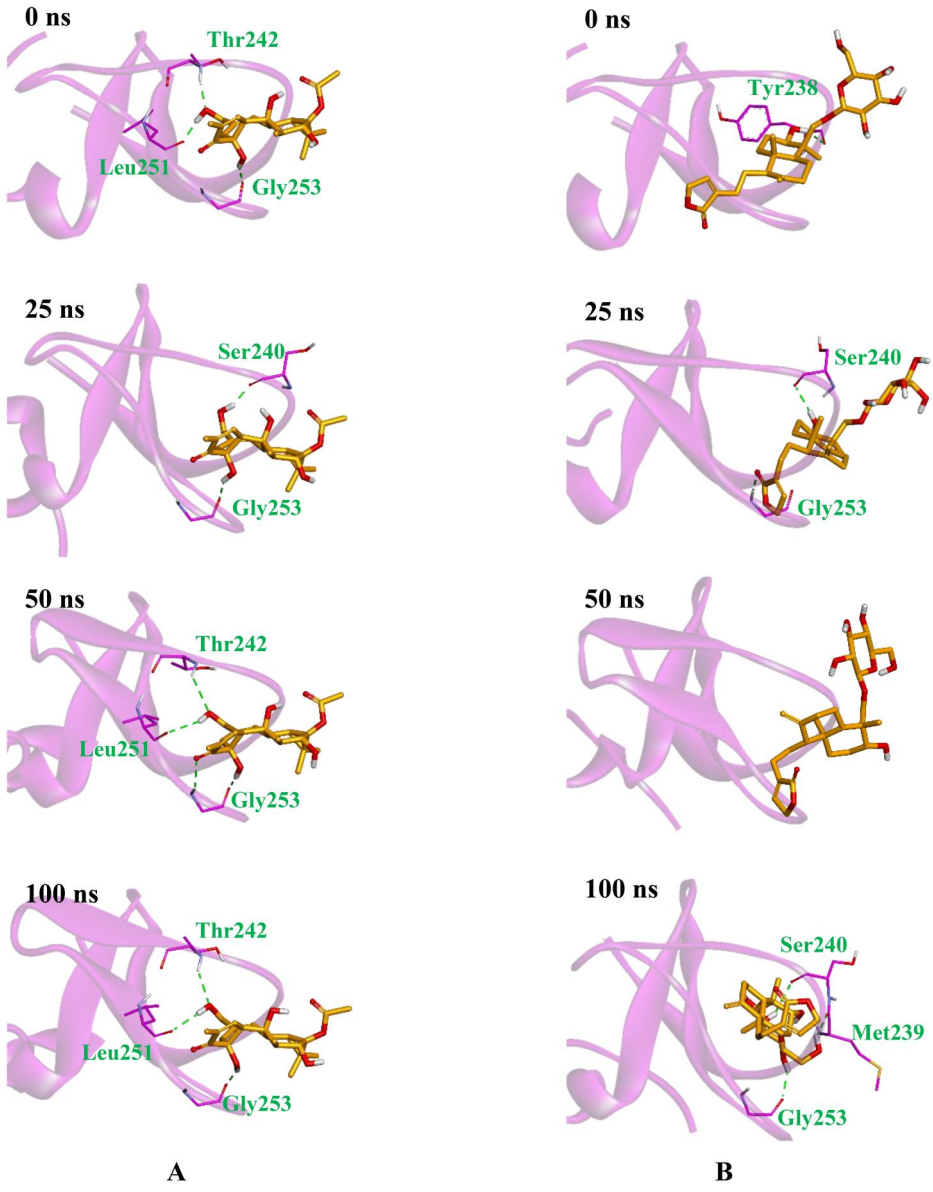

Figure 10. Interaction profiles of native ligand (A) and ninandrographolide (B) on PRKCD during MD simulations.

ligand-protein complexes followed by rescoring the binding free energy to obtain more accurate results. As shown in Table 6, all the potential compounds have a total binding energy similar to that of their native ligand. Among them, only 3-O-β-D-glucopyranosylandrographolide has more negative energy than the native ligand and this is in agreement with the consensus score from docking results.

Based on backbone (Cα) root mean square deviation (RMSD) profiles (Figure 7), all complexes appeared stable during the simulations indicating that the potential compounds, like the native ligands, did not cause significant changes to their respective targets. This was also observed in the root means square fluctuation (RMSF) analysis. As shown in Figure 8, there was no significant difference between the potential compound and native ligand in each target indicating that they affect the targets at a similar level, except for the native ligand-PTPN1 complex, the region around residue 116 was quite different from that of the potential compound-PTPN1 complex but this region does not include the active site. Nevertheless, the potential compounds and the native ligand revealed differences in behavior during the simulations which can be observed from their ligand RMSD (Figure 7) and interaction profiles (Figures 9–11).

In IKBKB, the native ligand appeared to be able to maintain its initial conformation (docking pose) during simulation. It was equilibrated at ± 0.2 nm since the beginning of the simulation (Figure 7A). From the interaction profile of the native ligand (Figure 9A), we identified Glu97, Cys99, Glu149, and Asn150 were the key residues. Meanwhile, 7-O-methyl wogonin was stable in RMSD values of ± 0.5 nm after 20 ns. Figure 9B revealed that its conformation at 25 ns changes slightly with the addition of two hydrogen bonds (H-bonds) compared to the docking pose (0 ns). We noticed that Cys99, Lys44, and Asp166 might be the important residues for this compound as they were always present in almost all sampled conformations. Several natural products from the flavonoid group such as naringenin, pinocembrin, and eriodictyol which have IKBKB suppressive activity were reported

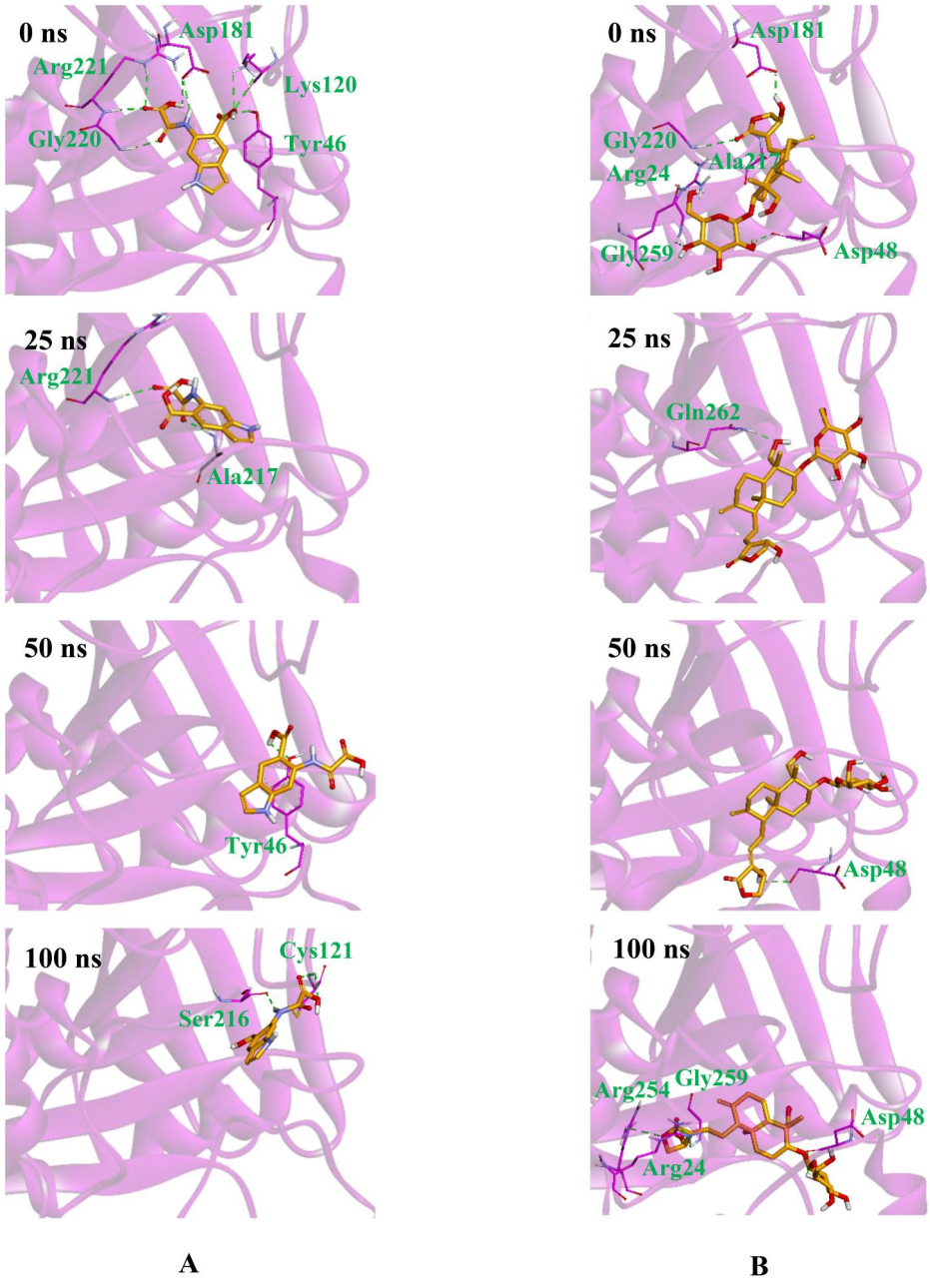

Figure 11. Interaction profiles of native ligand (A) and 3-O-β-D-glucopyranosyl andrographolide (B) on PTPN1 during MD simulations.

to interact with Cys99, and Asp166 through H-bonds (Zhang et al., 2023). Moreover, a study that evaluated the selectivity of a series of 4-substituted 2-amino-5-cyanopyrrolo[2,3-d]pyrimidines against IKK isoforms revealed that compounds that form H-bonds with Lys44 effectively have a greater affinity for IKBKB (Anthony et al., 2017). Overall, the interaction profile of 7-O-methyl wogonin demonstrated that it was stable at the binding site during the simulation.

In PRKCD, the native ligand was strongly anchored in the binding site as seen in the ligand RMSD (Figure 7B) and interaction profiles (Figure 10A). It was equilibrated from the beginning to the end of the simulation at ± 0.2 nm. This is confirmed by the interaction profiles where there were no significant changes in conformation during the simulations. Ser240, Thr242, Leu251, and Gly253 were the key residues observed in sampled conformations. In contrast to the native ligand, ninandrographolide showed a fluctuating RMSD profile in the first ± 70 ns before stabilizing at ± 0.75 nm. It was observed that this compound underwent a conformational change as seen from the interaction profile (Figure 10B). The docking pose (0 ns) showed one H-bond with Tyr238 and it was slightly different from the conformation at 25 ns. At 50 ns, no H-bonds were formed, and at 100 ns this compound rotated ± 90° but it formed three H-bonds with Met239, Ser240, and Gly253. The last two were the key residues as found in the native ligand's profile that also formed H-bonds at 25 ns. This confirmed that during the simulations ninandrographolide also remained on the binding site.

In PTPN1, 3-O-β-D-glucopyranosyl andrographolide showed a better ligand RMSD profile than the native ligand. As shown in Figure 7C, 3-O-β-D-glucopyranosyl andrographolide appears to reach equilibrium starting from ± 5 ns at ± 1 nm.

Meanwhile, the native ligand continues to fluctuate until the end of the simulation. This might be the reason why this native ligand needs to be further optimized to increase its affinity (Andersen et al., 2000). Nevertheless, as shown in Figure 11A, this native ligand remained in the active site of PTPN1 consisting of the P loop (His214-Arg221), WPD loop (Thr177-Pro185), and several residues such as Tyr46, Arg47, Val49, Lys120, Phe182, and Gln262 (Baskaran et al., 2012). Based on the interaction profile (Figure 11B), Asp48 was frequently found (at 0, 50, and 100 ns) to interact with 3-O-β-D-glucopyranosyl andrographolide. A study revealed that H-bonds with this residue were proven to be essential for better inhibition of PTP1B (Wan et al., 2006). From the sampled conformations, this compound was also found to form H-bonds with other residues such as Arg24, Asp181, Ala217, Gly220, Arg254, Gly259, and Gln262. Even though there was a conformational change that appears to be rotating, this interaction profile demonstrated that 3-O-β-D-glucopyranosyl andrographolide remained on the binding site.

4. Conclusion

FAPAC at 2 μg/mL significantly increased glucose uptake on IR-HepG2 cells. This formula may work to improve IR primarily by affecting inflammatory processes *via* IKBKB and insulin signal transduction mediated by PTPN1 and PRKCD. This formula promises to be developed as an insulin-sensitizing agent for T2DM treatment. However, further *in vitro* and *in vivo* studies are required to verify the activity of FAPAC against the main target.

Authors contributions

Conceptualization and methodology: FS, SN, KA, MC. Extract preparation: SR. *In vitro* assay: SAK, NN, AAF. Network pharmacology: FS. Docking simulation: FS, KB. Dynamics simulation: AA. Drafting manuscript: FS, SN, SAK, KA. All authors have read and approved the manuscript. All authors have an equal contributorship.

Disclosure statement

This research was conducted in collaboration with an industry partner, PT Soho Industri Pharmasi. The industry partner had no influence on the data collection and analysis, result interpretation, or manuscript writing. All scientific decisions were made entirely independently by the authors. There are no relevant financial or non-financial competing interests related to this manuscript.

Funding

This research activity is supported through RIIM Kompetisi funding from the Indonesia Endowment Fund for Education Agency, Ministry of Finance of the Republic of Indonesia and National Research and Innovation Agency (BRIN) of Indonesia according to the contract number: 78/II.7/HK/2022. We also thanks to the Research Organization for Health-BRIN for supporting this research activities.

References

Allen, W. J., Balius, T. E., Mukherjee, S., Brozell, S. R., Moustakas, D. T., Lang, P. T., Case, D. A., Kuntz, I. D., & Rizzo, R. C. (2015). DOCK 6: Impact of new features and current docking performance. *Journal of Computational Chemistry*, *36*(15), 1132–1156. https://doi.org/10.1002/jcc.23905

Andersen, H. S., Iversen, L. F., Jeppesen, C. B., Branner, S., Norris, K., Rasmussen, H. B., Møller, K. B., & Møller, N. P. (2000). 2-(oxalylamino)-benzoic acid is a general, competitive inhibitor of protein-tyrosine phosphatases. *The Journal of Biological Chemistry*, *275*(10), 7101–7108. https://doi.org/10.1074/jbc.275.10.7101

Anthony, N. G., Baiget, J., Berretta, G., Boyd, M., Breen, D., Edwards, J., Gamble, C., Gray, A. I., Harvey, A. L., Hatziieremia, S., Ho, K. H., Huggan, J. K., Lang, S., Llona-Minguez, S., Luo, J. L., McIntosh, K., Paul, A., Plevin, R. J., Robertson, M. N., … Mackay, S. P. (2017). Inhibitory Kappa B Kinase α (IKKα) inhibitors that recapitulate their selectivity in cells against isoform-related biomarkers. *Journal of Medicinal Chemistry*, *60*(16), 7043–7066. https://doi.org/10.1021/acs.jmedchem.7b00484

Arkan, M. C., Hevener, A. L., Greten, F. R., Maeda, S., Li, Z. W., Long, J. M., Wynshaw-Boris, A., Poli, G., Olefsky, J., & Karin, M. (2005). IKK-β links inflammation to obesity-induced insulin resistance. *Nature Medicine*, *11*(2), 191–198. https://doi.org/10.1038/nm1185

Arslanian, S., Pyle, L., Payan, M., Bacha, F., Caprio, S., Haymond, M. W., Levitsky, L. L., Goland, R., White, N. H., & Willi, S. M. (2013). Effects of metformin, metformin plus rosiglitazone, and metformin plus lifestyle on insulin sensitivity and -βcell function in TODAY. *Diabetes Care*, *36*(6), 1749–1757. https://doi.org/10.2337/dc12-2393

Bai, H., Wang, R., Li, Y., Liang, X., Zhang, J., Sun, N., & Yang, J. (2022). Network pharmacology analysis, molecular docking, and in vitro verification reveal the action mechanism of *Prunella vulgaris* L. in treating breast cancer. *Evidence-Based Complementary and Alternative Medicine*, *2022*, 5481563. https://doi.org/10.1155/2022/5481563

Baskaran, S. K., Goswami, N., Selvaraj, S., Muthusamy, V. S., & Lakshmi, B. S. (2012). Molecular dynamics approach to probe the allosteric inhibition of PTP1B by chlorogenic and cichoric acid. *Journal of Chemical Information and Modeling*, *52*(8), 2004–2012. https://doi.org/10.1021/ci200581g

Burgos, R. A., Alarcón, P., Quiroga, J., Manosalva, C., & Hancke, J. (2020). Andrographolide, an anti-inflammatory multitarget drug: All roads lead to cellular metabolism. *Molecules*, *26*(1), 5. https://doi.org/10.3390/molecules26010005

Chang, C. L. T., Lin, Y., Bartolome, A. P., Chen, Y. C., Chiu, S. C., & Yang, W. C. (2013). Herbal therapies for type 2 diabetes mellitus: Chemistry, biology, and potential application of selected plants and compounds. *Evidence-Based Complementary and Alternative Medicine*, *2013*, 378657. https://doi.org/10.1155/2013/378657

Cui, X., Qian, D. W., Jiang, S., Shang, E. X., Zhu, Z. H., & Duan, J. A. (2018). Scutellariae radix and coptidis rhizoma improve glucose and lipid metabolism in T2DM rats via regulation of the metabolic profiling and MAPK/PI3K/Akt signaling pathway. *International Journal of Molecular Sciences*, *19*(11), 3634. https://doi.org/10.3390/ijms19113634

Galicia-Garcia, U., Benito-Vicente, A., Jebari, S., Larrea-Sebal, A., Siddiqi, H., Uribe, K. B., Ostolaza, H., & Martín, C. (2020). Pathophysiology of type 2 diabetes mellitus. *International Journal of Molecular Sciences*, *21*(17), 6275. https://doi.org/10.3390/ijms21176275

Gfeller, D., Grosdidier, A., Wirth, M., Daina, A., Michielin, O., & Zoete, V. (2014). SwissTargetPrediction: A web server for target prediction of bioactive small molecules. *Nucleic Acids Research*, *42*, W32–W38. https://doi.org/10.1093/nar/gku293

Hess, B., Kutzner, C., Van Der Spoel, D., & Lindahl, E. (2008). GRGMACS 4: Algorithms for highly efficient, load-balanced, and scalable molecular simulation. *Journal of Chemical Theory and Computation*, *4*(3), 435–447. https://doi.org/10.1021/ct700301q

Hu, X., Wang, S., Xu, J., Wang, D.-B., Chen, Y., & Yang, G.-Z. (2014). Triterpenoid saponins from stauntonia chinensis ameliorate insulin resistance via the amp-activated protein kinase and IR/IRS-1/PI3K/Akt pathways in insulin-resistant HepG2 cells. *International Journal of Molecular Sciences*, *15*(6), 10446–10458. https://doi.org/10.3390/ijms150610446

Lee, S. H., Park, S. Y., & Choi, C. S. (2022). Insulin resistance: From mechanisms to therapeutic strategies. *Diabetes & Metabolism Journal*, *46*(1), 15–37. https://doi.org/10.4093/Dmj.2021.0280

Li, M., Chi, X., Wang, Y., Setrerrahmane, S., Xie, W., & Xu, H. (2022). Trends in insulin resistance: Insights into mechanisms and therapeutic strategy. *Signal Transduction and Targeted Therapy*, *7*(1), 216. https://doi.org/10.1038/s41392-022-01073-0

Li, M., Vienberg, S. G., Bezy, O., O'Neill, B. T., & Kahn, C. R. (2015). Role of PKCδ in insulin sensitivity and skeletal muscle metabolism. *Diabetes*, *64*(12), 4023–4032. https://doi.org/10.2337/db14-1891/-/dc1

Liu, H. W., Huang, W. C., Yu, W. J., & Chang, S. J. (2015). Toona sinensis ameliorates insulin resistance via AMPK and PPARγ pathways. *Food & Function*, *6*(6), 1855–1864. https://doi.org/10.1039/c5fo00056d

Liu, Y., Li, X., Xie, C., Luo, X., Bao, Y., Wu, B., Hu, Y., Zhong, Z., Liu, C., & Li, M. J. (2016). Prevention effects and possible molecular mechanism of mulberry leaf extract and its formulation on rats with insulin-insensitivity. *PLOS One*, *11*(4), e0152728. https://doi.org/10.1371/journal.pone.0152728

Ma, Y. M., Tao, R. Y., Liu, Q., Li, J., Tian, J. Y., Zhang, X. L., Xiao, Z. Y., & Ye, F. (2011). PTP1B inhibitor improves both insulin resistance and lipid abnormalities in vivo and in vitro. *Molecular and Cellular Biochemistry*, *357*(1–2), 65–72. https://doi.org/10.1007/s11010-011-0876-4

Mastrototaro, L., & Roden, M. (2021). Insulin resistance and insulin sensitizing agents. *Metabolism: Clinical and Experimental*, *125*, 154892. https://doi.org/10.1016/j.metabol.2021.154892

Mosmann, T. (1983). Rapid colorimetric assay for cellular growth and survival: Application to proliferation and cytotoxicity assays. *Journal of Immunological Methods*, *65*(1–2), 55–63. https://doi.org/10.1016/0022-1759(83)90303-4

Ng, Y. L., Salim, C. K., & Chu, J. J. H. (2021). Drug repurposing for COVID-19: Approaches, challenges and promising candidates. *Pharmacology & Therapeutics*, *228*, 107930. https://doi.org/10.1016/j.pharmthera.2021.107930

Noor, F., Qamar, M. T. U., Ashfaq, U. A., Albutti, A., Alwashmi, A. S. S., & Aljasir, M. A. (2022). Network pharmacology approach for medicinal plants: Review and assessment. *Pharmaceuticals*, *15*(5), 572. https://doi.org/10.3390/ph15050572

Oliveira, T. A. D., Silva, M. P. D., Maia, E. H. B., Silva, A. M. D., & Taranto, A. G. (2023). Virtual screening algorithms in drug discovery: A review focused on machine and deep learning methods. *Drugs and Drug Candidates*, *2*(2), 311–334. https://doi.org/10.3390/ddc2020017

Panahi, G., Pasalar, P., Zare, M., Rizzuto, R., & Meshkani, R. (2018). High glucose induces inflammatory responses in HepG2 cells via the oxidative stress-mediated activation of NF-κB, and MAPK pathways in HepG2 cells. *Archives of Physiology and Biochemistry*, *124*(5), 468–474. https://doi.org/10.1080/13813455.2018.1427764

Pantsar, T., & Poso, A. (2018). Binding affinity via docking: Fact and fiction. *Molecules*, *23*(8), 1899. https://doi.org/10.3390/molecules23081899

Panzhinskiy, E., Ren, J., & Nair, S. (2013). Pharmacological inhibition of protein tyrosine phosphatase 1b: A promising strategy for the treatment of obesity and type 2 diabetes mellitus. *Current Medicinal Chemistry*, *20*(21), 2609–2625. https://doi.org/10.2174/0929867311320210001

Sangande, F., Agustini, K., & Budipramana, K. (2023). Antihyperlipidemic mechanisms of a formula containing *Curcuma xanthorrhiza*, *Sechium edule*, and *Syzigium polyanthum*: In silico and in vitro studies. *Computational Biology and Chemistry*, *105*, 107907. https://doi.org/10.1016/j.compbiolchem.2023.107907

Shehadeh, M. B., Suaifan, G. A. R. Y., & Abu-Odeh, A. M. (2021). Plants secondary metabolites as blood glucose-lowering molecules. *Molecules*, *26*(14), 4333. https://doi.org/10.3390/molecules26144333

Singh, S., Singh Grewal, A., Grover, R., Sharma, N., Chopra, B., Kumar Dhingra, A., Arora, S., Redhu, S., & Lather, V. (2022). Recent updates on development of protein-tyrosine phosphatase 1B inhibitors for treatment of diabetes, obesity and related disorders. *Bioorganic Chemistry*, *121*, 105626. https://doi.org/10.1016/j.bioorg.2022.105626

Suemanotham, N., Phochantachinda, S., Chatchaisak, D., Sakcamduang, W., Chansawhang, A., Pitchakarn, P., & Chantong, B. (2023). Antidiabetic effects of *Andrographis paniculata* supplementation on biochemical parameters, inflammatory responses, and oxidative stress in canine diabetes. *Frontiers in Pharmacology*, *14*, 1077228. https://doi.org/10.3389/fphar.2023.1077228

Sulfianti, A., Firdausi, N., Nurhadi, N., Ngatinem, N., Agustini, K., & Ningsih, S. (2023). Antidiabetic activity of *Anredera cordifolia* (Ten.) Stennis extracts with different ethanol percentages: An evaluation based on in vitro, in vivo, and molecular studies. *Pharmacia*, *70*(1), 39–47. https://doi.org/10.3897/pharmacia.70.e94899

Trott, O., & Olson, A. J. (2010). AutoDock Vina: Improving the speed and accuracy of docking with a new scoring function, efficient optimization, and multithreading. *Journal of Computational Chemistry*, *31*(2), 455–461. https://doi.org/10.1002/jcc.21334

Urzua, A., Semple, S., Tam, Y. K., Wei, J., Li, J., Bai, L., Wei, F., Zhao, J., Wang, D., Xiao, Y., & Yan, W. (2019). Therapeutic mechanisms of herbal medicines against insulin resistance: A review. *Frontiers in Pharmacology*, *10*, 661. https://doi.org/10.3389/fphar.2019.00661

Vaou, N., Stavropoulou, E., Voidarou, C., Tsakris, Z., Rozos, G., Tsigalou, C., & Bezirtzoglou, E. (2022). Interactions between medical plant-derived bioactive compounds: Focus on antimicrobial combination effects. *Antibiotics*, *11*(8), 1014. https://doi.org/10.3390/antibiotics11081014

Wan, Z. K., Lee, J., Xu, W., Erbe, D. V., Joseph-McCarthy, D., Follows, B. C., & Zhang, Y. L. (2006). Monocyclic thiophenes as protein tyrosine phosphatase 1B inhibitors: Capturing interactions with Asp48. *Bioorganic & Medicinal Chemistry Letters*, *16*(18), 4941–4945. https://doi.org/10.1016/j.bmcl.2006.06.051

Yang, S. J., Choi, J. M., Park, S. E., Rhee, E. J., Lee, W. Y., Oh, K. W., Park, S. W., & Park, C. Y. (2015). Preventive effects of bitter melon (*Momordica charantia*) against insulin resistance and diabetes are associated with the inhibition of NF-κB and JNK pathways in high-fat-fed OLETF rats. *The Journal of Nutritional Biochemistry*, *26*(3), 234–240. https://doi.org/10.1016/j.jnutbio.2014.10.010

Yao, J., Zhao, L., Zhao, Q., Zhao, Y., Sun, Y., Zhang, Y., Miao, H., You, Q. D., Hu, R., & Guo, Q. L. (2014). NF-κB and Nrf2 signaling pathways contribute to wogonin-mediated inhibition of inflammation-associated colorectal carcinogenesis. *Cell Death & Disease*, *5*(6), e1283–e1283. https://doi.org/10.1038/cddis.2014.221

Zhang, J., Zhang, R., Li, W., Ma, X.-C., Qiu, F., & Sun, C.-P. (2023). IκB kinase β (IKKβ): Structure, transduction mechanism, biological function, and discovery of its inhibitors. *International Journal of Biological Sciences*, *19*(13), 4181–4203. https://doi.org/10.7150/ijbs.85158

Zhao, L., Zhang, H., Li, N., Chen, J., Xu, H., Wang, Y., & Liang, Q. (2023). Network pharmacology, a promising approach to reveal the pharmacology mechanism of Chinese medicine formula. *Journal of Ethnopharmacology*, *309*, 116306. https://doi.org/10.1016/j.jep.2023.116306

Zhao, M., Fu, L., Xu, P., Wang, T., & Li, P. (2023). Network pharmacology and experimental validation to explore the effect and mechanism of Kanglaite injection against triple-negative breast cancer. *Drug Design, Development and Therapy*, *17*, 901–917. https://doi.org/10.2147/dddt.s397969

Zhao, X., An, X., Yang, C., Sun, W., Ji, H., & Lian, F. (2023). The crucial role and mechanism of insulin resistance in metabolic disease. *Frontiers in Endocrinology*, *14*, 1149239. https://doi.org/10.3389/fendo.2023.1149239